PNAS RESEARCH ARTICLE | GENETICS OPEN ACCESS

The deubiquitinase Usp7 in *Drosophila melanogaster* is required for synaptonemal complex maintenance

Cathleen M. Lake[a], Jennifer Gardner[a], Salam Briggs[a], Zulin Yu[a], Grace McKown[a], and R. Scott Hawley[a,b,1]

Contributed by R. Scott Hawley; received May 10, 2024; accepted July 23, 2024; reviewed by Nicole Crown, Hiroyuki Ohkura, and Ofer Rog

Meiosis is a form of cell division that is essential to sexually reproducing organisms and is therefore highly regulated. Each event of meiosis must occur at the correct developmental stage to ensure that chromosomes are segregated properly during both meiotic divisions. One unique meiosis-specific structure that is tightly regulated in terms of timing of assembly and disassembly is the synaptonemal complex (SC). While the mechanism(s) for assembly and disassembly of the SC are poorly understood in *Drosophila melanogaster*, posttranslational modifications, including ubiquitination and phosphorylation, are known to play a role. Here, we identify a role for the deubiquitinase Usp7 in the maintenance of the SC in early prophase and show that its function in SC maintenance is independent of the meiotic recombination process. Using two *usp7* shRNA constructs that result in different knockdown levels, we have shown that the presence of SC through early/mid-pachytene is critical for normal levels and placement of crossovers.

meiosis | SC | deubiquitinase | DUB | Usp7

Significance

We provide evidence that the deubiquitinase, Usp7, is required for the maintenance of the synaptonemal complex (SC) in early meiotic prophase I in *Drosophila melanogaster*. These studies identify a critical time point in prophase I, the transition from early to early/mid-pachytene, that the SC structure is important for the proper disjunction of meiotic chromosomes. In addition, these studies also support previous work from our laboratory in suggesting that the presence of SC throughout early/mid-pachytene is required for the proper number and placement of crossovers, affecting the *X* chromosome differently than the autosomes.

The process of chromosome segregation during meiosis is tightly regulated to ensure the proper transmission of chromosomes to the gametes. There are many aspects of meiotic regulation, including transcriptional regulation, regulation of the timing and order of key events, meiotic checkpoints that regulate progression, and entry and exit regulation throughout many stages of meiosis, just to name a few. The failure to properly regulate and execute these processes can lead to chromosome segregation errors. Missegregation of chromosomes at meiosis I and/or II results in aneuploid gametes, which is the leading cause of miscarriages and birth defects in humans (1).

A complex process unique to the meiotic cell cycle is the induction of a large number of preprogrammed double-strand breaks (DSBs) that are repaired by homologous recombination. This process results in chiasmata, the physical manifestation of crossovers, which ensure the segregation of homologous chromosomes during the first meiotic division. Homologous recombination, which occurs in prophase I, is facilitated by a series of events that includes the building a meiosis-specific structure (the synaptonemal complex, SC) which connects the homologs along their entire length, the induction of DSBs, and the repair of those breaks into crossovers and noncrossovers or gene conversions. These events are critical to ensure not only the proper timing of each event but also that none of the events are missed. For example, failure to build or maintain the SC throughout crossover formation results in defects that include chromosome segregation errors, misplacement of crossovers, and/or alterations in crossover number (2–4). There are a number of factors that regulate DSB timing, number, and distribution (5). In some organisms, failure to induce DSBs will cause meiotic arrest (6, 7), while in others, like female flies, the loss of DSBs leads only to elevated levels of chromosome missegregation. In *Drosophila melanogaster*, where DSB induction occurs after SC formation, the SC is required for wild-type levels of DSBs, and those DSBs that do form in the absence of SC are rarely resolved into crossovers (8–10).

Therefore, in *Drosophila*, knowledge of both the mechanisms that control the timing of SC formation and the maintenance of SC throughout early stages of prophase I will be required to understand many aspects of meiotic chromosome behavior. Unfortunately, most prior studies of this process have been done using null mutations in genes that encode crucial SC components, and thus, the regulation of SC formation and maintenance is not well understood. However, a few studies have recently shed some light on the regulation of SC assembly and maintenance. These studies have implicated posttranslational modifications as important factors in SC assembly and maintenance. While no direct role for ubiquitin has been identified in *Drosophila* females, indirect evidence suggests that ubiquitination may play a role in many processes of meiotic prophase. For example, several recent studies have shown that both ubiquitination and phosphorylation are important for controlling SC dynamics. A known E3 ubiquitin ligase, Sina, has been shown to

Author affiliations: [a]Stowers Institute for Medical Research, Kansas City, MO 64110; and [b]Department of Molecular and Integrative Physiology, University of Kansas Medical Center, Kansas City, KS 66160

Author contributions: C.M.L., J.G., and R.S.H. designed research; C.M.L., J.G., S.B., Z.Y., and G.M. performed research; C.M.L. contributed new reagents/analytic tools; C.M.L., J.G., S.B., G.M., and R.S.H. analyzed data; and C.M.L. and R.S.H. wrote the paper.

Reviewers: N.C., Case Western Reserve University; H.O., University of Edinburgh; and O.R., The University of Utah.

The authors declare no competing interest.

[1]To whom correspondence may be addressed. Email: rsh@stowers.org.

This article contains supporting information online at https://www.pnas.org/lookup/suppl/doi:10.1073/pnas.2409346121/-/DCSupplemental.

Published August 27, 2024.

regulate SC formation and disassembly (11). A point mutation in the dimerization domain of *sina* causes aberrant formation of SC structures known as polycomplexes (PCs), which can persist past the developmental stage when the euchromatic SC has disassembled. On the other hand, another ubiquitin ligase complex, SCF-Fbox42, has been shown to promote SC assembly by downregulating PP2A-B56 (12), showing that there is a cooperation between ubiquitination and phosphorylation for SC assembly and maintenance in *Drosophila*. Finally, there is a second SCF complex (SCF-Slimb/βTrcp) that, along with SCF-Fbxo42, mediates regulation of the SC (12). Both complexes showed impaired assembly and premature disassembly of the SC, as well as abnormal karyosome morphologies.

Studies in other organisms also support the view that ubiquitination-related processes play important roles in building and dismantling the SC. In budding yeast, studies have identified a direct role for ubiquitin, having both positive and negative roles, in SC formation and limiting the number of DSBs that occur (13). In addition, in mice, the process of ubiquitination is important in assuring the timely degradation of a SC axial element protein, SYCP3, which is necessary to ensure DSB repair at pachytene (14). Ubiquitination, which affects protein localization, stability, interactions, and activity, is often itself regulated by enzymes known as DUBs, or deubiquitinating enzymes. DUBs reverse the ubiquitin marks, and therefore, DUBs could be equally important for maintaining protein stability, localization, or activity. There are 100s of DUBs in the genomes of most organisms; however, the most extensively studied is the ubiquitin-specific protease 7 (Usp7) due to its numerous substrates and the many roles it has in protecting the genome (15–17).

To further investigate the role of ubiquitination on processes relating to the SC in *Drosophila*, we asked whether the DUB Usp7 had a role in early meiotic prophase. We found that reducing the expression of *usp7* in the female germline led to a failure to maintain the SC throughout pachytene. In this study, we demonstrate, using two shRNA constructs to *usp7* that differ in their ability to knockdown *usp7* expression, that the presence of the SC through early/mid-pachytene is critical for normal levels and placement of crossovers. We also find that an intact SC, specifically at the transition from early to early/mid-pachytene, is critical for the disjunction of even those meiotic chromosomes that have undergone crossing over. We show that the failure to maintain the SC is independent of the meiotic recombination process and that Usp7 may be interacting directly with a component of the SC. These studies identify a unique role for the deubiquitinase Usp7 in maintaining the structure of the SC throughout meiotic prophase I.

Results

The Efficacy of the *usp7* Knockdown Constructs in the Female Germline. Ubiquitination is a process that can affect the localization, stability, interactions, and activity of proteins, and deubiquitination can reverse these effects. Since recent studies have determined that enzymes responsible for ubiquitination affect the SC, we wanted to determine the consequences of impairing the processes that mediate deubiquitination. While there are many deubiquitinases within the genome of most species, Usp7 (also known as Herpesvirus-associated ubiquitin specific protease or HUASP) is the most extensively studied due to its many roles in maintaining genome integrity (17). We investigated whether Usp7 was required during *Drosophila* female meiosis for events related to meiotic prophase I.

In *D. melanogaster*, the gene that encodes Usp7 (*usp7*) is an essential gene located on the *X* chromosome. A small deletion mutation of this gene, created by CRISPR-Cas9, caused homozygotes to die prematurely at the pupal stage (18), and both a deficiency that uncovers *usp7* and an available P-element mutation are male lethal, making it impossible to create homozygous null females (Table 1). Most studies relating to *usp7* in *Drosophila* have been done using a shRNA line targeting the 3'UTR generated by the Transgenic RNAi Project (TRiP) (BL34708) (19) in which expression can be reduced in a specific tissue of interest. Previous studies using this TRiP shRNA line, which is located on Chr3 and denoted as *usp7 RNAi^{III}* for this study, showed knockdown of expression levels to approximately 70% and 80% of wildtype levels using a steroid inducible ubiquitous *daughterless-geneswitch-Gal4* or neuron specific (*D42*)-*Gal4* driver, respectively (20). Even at this level of reduction within the tissue, effects were seen in the ability of flies to adapt to stress conditions and proteotoxicity in neurons. In addition to this shRNA line, we made a second shRNA line targeting the first exon of *usp7* using the same vector (pValium20) and inserted the construct on Chr2 (denoted *usp7 RNAi^{II}*) (*Materials and Methods*).

We tested both of the shRNA constructs for their ability to reduce *usp7* expression in the germarium when combined with the germline-specific *nanos-Gal4* driver which is expressed robustly in the stem cells and meiotic cells in both females and males (21, 22). The use of this driver causes the *usp7* transcript to be expressed normally in the supporting somatic cells while being reduced only in the meiotic germline. A qPCR analysis indicated that *usp7 RNAi^{II}* reduced expression of *usp7* transcript in the ovary to between 43 and 47% of wildtype levels (a reduction of greater than 50%) and *usp7 RNAi^{III}* reduced expression to between 85 and 90% of wildtype levels (a reduction of 10 to 15%) (*SI Appendix*, Fig. S1). As whole ovaries were used in this assay, the effect of *usp7* knockdown within the germline cells was likely greater than observed for the whole ovary. We conclude that *usp7 RNAi^{II}* was the better tool for reducing *usp7* expression in the female germline, and the reduced level of expression of *usp7 RNAi^{III}* is similar to what has been reported for other tissue-specific knockdowns.

Since *usp7* is an essential gene and even a 20 to 30% reduction driven by tissue-specific knockdown showed phenotypes in other studies, we asked whether or not using *usp7 RNAi^{II}* and *usp7 RNAi^{III}* to reduce the expression of *usp7* in the germline would

Table 1. *usp7* mutant fertility phenotype

Genotype	Vector	Location of hairpin	Fertility of females[†]	Fertility of males[†]
PSUP or Pusp7[KG06814]	n/a[*]	n/a	n/a	Lethal
Df(1)ED7161	n/a	n/a	n/a	Lethal
nanos-Gal4::VP16/+; usp7RNAi^{II}/+	pValium20	1st exon	Semi-fertile	Virtually sterile
nanos-Gal4::VP16/+;; usp7RNAi^{III}/+	pValium20	3'UTR	Fertile	Fertile

PSUP or Pusp7[KG06814] is a transgenic insertion stock created by the Gene Disruption project (Bloomington Stock 14505). *Df(1)ED7161* was created by the DrosDel Project and deletes numerous genes, including *usp7*, between cytological positions 11A1;11B14 (Bloomington Stock 9217).
[*]Not applicable.
[†]Refer to *SI Appendix*, Table S1 for average number of progeny per fly.

impair fertility (Table 1 and *SI Appendix*, Table S1). We found that while *usp7 RNAi*^{III} knockdown in both the female and male germlines resulted in fertile progeny comparable to controls, knockdown using *usp7 RNAi*^{II} resulted in a significant decrease in fertility of females and virtual sterility in the males. The stronger effect on fertility in *usp7 RNAi*^{II} compared to *usp7 RNAi*^{III} is consistent with this line having a greater level of knockdown in *usp7* expression within the whole ovary. The decrease in female fertility was due to reduced expression in the germline, as in no defect was observed in the absence of driver (*SI Appendix*, Table S1). When we used the *maternal-α-Gal4* driver (called *matα-Gal4*), which drives expression of the shRNA after early meiotic prophase events (starting in germarial stage 3/vitellarium stage 2, see *SI Appendix*, Fig. S2) and continues throughout oogenesis (22–25), we observed a similar decrease in female fertility for *usp7 RNAi*^{II} compared to the *nanos-Gal4* driver (*SI Appendix*, Table S1). This observation suggests that the decrease in fertility is mostly due to an effect of knockdown at a point in development past the early meiotic events in the germarium.

Reduction of *usp7* Expression Leads to a SC Maintenance Phenotype. We next tested whether knockdown of *usp7* expression altered those early events in female meiotic prophase that have been most thoroughly characterized for *D. melanogaster* females. Within the ovary, the ovarioles are arranged in a linear fashion by developmental age, and the timing of events can be analyzed cytologically. In addition, progeny that are produced from mated females can be analyzed for various meiotic defects, including failed chromosome segregation or recombination defects. The timing of the meiotic events relevant to this study is shown in *SI Appendix*, Fig. S2. Meiosis begins after the formation of the 16-cell cyst, where SC begins to form in several cells within the cyst in early pachytene. Following punctate SC loading, full-length SC formation can be seen before the induction of DSBs which are visualized with a marker to a posttranslational modification on the histone 2A variant (γH2Av). As the cyst matures and moves posteriorly in the germarium, the γH2Av foci number decreases until it reaches near zero at the posterior end of the germarium in the selected oocyte. This gradual reduction of γH2Av number indicates that DSB repair is underway and/or complete before the cyst exits the germarium, producing the first vitellarium egg chamber. As the egg chamber matures posteriorly, the SC begins to disassemble along the euchromatic arms but is maintained at the centromeres where it is thought to aid in chromosome alignment at metaphase I.

We first analyzed whether *usp7* knockdown in the female germline affected the formation of the SC or the kinetics of SC assembly and disassembly. We visualized SC formation in the germarium from early pachytene through the beginning of mid-pachytene using an antibody to the SC transverse filament protein, C(3)G (Fig. 1*A*). We found that *usp7* knockdown by either *usp7 RNAi*^{II} or *usp7 RNAi*^{III} showed a defect in the ability to maintain the SC structure throughout pachytene in the germarium. In both cases, by the start of mid-pachytene (region 3), the last cyst within the germarium, only punctate foci of SC remained in most oocytes. This contrasts with the full-length SC observed in the control. Further analysis revealed that the SC maintenance defect in *usp7 RNAi*^{II} occurs earlier than *usp7 RNAi*^{III} (Fig. 1*B*). We found that the SC defect in *usp7 RNAi*^{II} was already apparent by early pachytene with only 77% of the nuclei having wild-type thread-like SC compared to both *usp7 RNAi*^{III} and the control, where 100% of the pro-oocyte nuclei had normal thread-like SC. In both *usp7 RNAi*^{II} and *usp7 RNAi*^{III} pro-oocytes, as the cyst matured throughout the germarium, the frequencies of SC maintenance defect increased, with both constructs causing complete or near complete disassembly of the SC by mid-pachytene (region 3) (100% of *usp7 RNAi*^{II} and 96% of *usp7 RNAi*^{III} nuclei have only fragments or spots of SC remaining).

We then used SIM to examine the structure of the SC at higher resolution in both *usp7 RNAi*^{II} and *usp7 RNAi*^{III} to detect any gross abnormality that could explain the premature disassembly or maintenance. Using antibodies that recognizes the lateral sides of the SC (C terminus C(3)G antibody) and a central region protein, Corolla, we found that the SC that forms in early pachytene looked structurally normal (*SI Appendix*, Fig. S3 *A–C*). In addition, we could see that in early/mid-pachytene some of the fragments/spots of SC in ovaries expressing either shRNA construct still retained

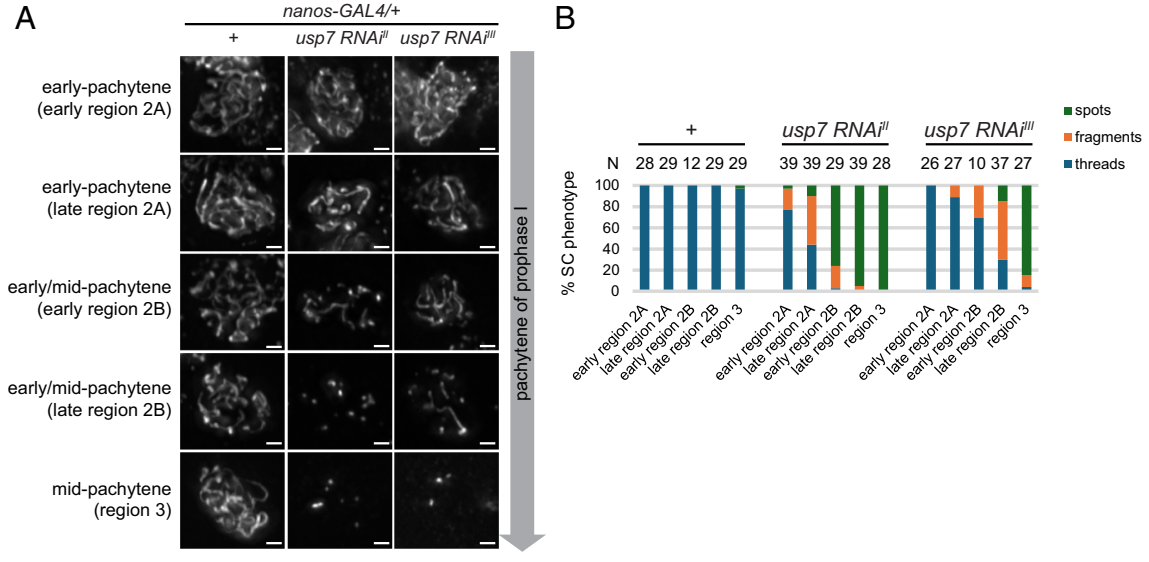

Fig. 1. Germline knockdown of *usp7* by RNAi results in failure to maintain the SC throughout pachytene. (*A*) Immunofluorescence analysis of nuclei in the germarium from early pachytene (region 2A) through mid-pachytene (region 3) in *y w nanos-Gal4/y sc cv v f·y+* with either no RNAi construct (+) or the indicated *usp7 RNAi* construct (*usp7 RNAi*^{II} or *usp7 RNAi*^{III}). Ovaries were stained with an antibody to C(3)G (white) to mark the SC. Region 2A and 2B pro-oocytes are categorized as early and late by position within the germarium. Images are maximum-intensity projections of the deconvolved *z*-series through the selected nuclei. (Scale bar, 1 μm.) (*B*) Quantification of the SC phenotype in *y w nanos-Gal4/y sc cv v f·y+* with either no RNAi construct (+) or the indicated *usp7 RNAi* construct throughout early pachytene (early and late region 2A), early/mid-pachytene (early and late region 2B), and mid-pachytene (region 3). N, number of nuclei analyzed.

tripartite structure with two lateral sides and a central element with similar interaxis distances. This indicates that the SC defect is not related to the inability to assemble structurally normal SC, but rather in the ability to stabilize or maintain the SC structure.

To determine whether the failure to maintain the SC was related to cohesion between the sister chromatids, we analyzed centromere clustering in *usp7 RNAi*^{II} and *usp7 RNAi*^{III} females (*SI Appendix*, Table S2). In *Drosophila*, centromeres of the eight chromosomes pair with their homolog and cluster into one to two aggregates by early pachytene and remain clustered throughout prophase I (26, 27). This active clustering of centromeres occurs primarily from the association of homologous chromosome interactions (27). Centromere pairing is dependent on cohesion, and centromere clustering is dependent on SC formation (26–31). We performed an immunofluorescence assay to determine whether defects in SC maintenance could be explained by potential defects in cohesion. We found that centromere pairing is not affected using either shRNA construct, as there were never greater than four centromere pairs, indicating that cohesion defects are likely not the cause of the failure to maintain the SC. Even at mid/late prophase, where the cohesion mutant, *ord*, shows a complete lack of centromere pairing (8 CID foci) (26), both *usp7* shRNA constructs maintain the ability to pair centromeres (3.8 CID foci for *usp7 RNAi*^{II} and 3.0 CID foci for *usp7 RNAi*^{III}). In addition, we found that there is only a mild effect on centromere clustering that is similar to the previously published null mutation in the *cona* gene, which encodes an SC structural component (4.3 CID foci at mid/late prophase) (26). However, we acknowledge that these studies cannot exclude potential defects in arm cohesion that are independent of cohesion at the centromeres.

We conclude from these studies that when *usp7* expression is reduced, the pro-oocytes fail to maintain the SC and that stronger reduction in *usp7* transcript is correlated with an earlier SC defect. We also note that the failure to maintain the SC structure is likely not due to a defect in cohesion or some gross abnormality in the ability to form the tripartite SC.

Effect of *usp7 RNAi* on Meiotic Crossing Over and Chromosome Segregation. To determine whether the failure to maintain the SC during these critical points in prophase I resulted in a change in recombination frequency or position, we assayed meiotic crossing over along the *X* chromosome (Table 2). This assay also allowed us to analyze nondisjunction (ND) levels of the *X* chromosome at the same time (see *Materials and Methods* for details). We found that crossing over within the *sc-f* region of the *X* chromosome in both *usp7 RNAi* females was reduced by approximately 60% compared to control. Crossover distribution on the *X* chromosome in *usp7 RNAi*^{II} oocytes was reduced in a nonuniform fashion, such that the centromere distal interval of *sc-cv* was affected to a lesser extent than the more proximal euchromatic interval of *cv-f*. However, crossovers in *usp7 RNAi*^{III} were reduced uniformly along the *X* chromosome. These differences in *X* chromosome crossover distribution between the two *usp7 RNAi* oocytes could be attributed to the poor fertility of *usp7 RNAi*^{II} oocytes and the possibility that some marker combinations could be more favorable than others. While the overall rate of *X* chromosome crossing over was similarly reduced in both *usp7 RNAi* females, we observed significant differences in the rate of *X* chromosome missegregation. *usp7 RNAi*^{II} oocytes exhibit a ninefold higher level of *X* ND than *usp7 RNAi*^{III} oocytes (35.1% *X* ND for *usp7 RNAi*^{II} compared to 4.4% in *usp7 RNAi*^{III}), although both ND levels are significantly increased compared to controls ($P < 0.001$) (32). However, both these results led us to speculate there could be differences in the effects of *usp7* reduction on the autosomes.

Because the ND of nonexchange *X* chromosomes observed in recombination-deficient mutants reflects nonhomologous segregation events, in which the two noncrossover *X* chromosomes segregate from a nonexchange autosome, this process by definition requires the presence of nonexchange autosomes (see below) (33). Thus, it seemed possible that the observed differences in the level of *X* ND might reflect a differential effect of the two constructs on autosomal crossing over. To test this possibility, we analyzed the crossover frequency and distribution on the *2nd* chromosome for *usp7 RNAi*^{III}. In this assay, we were able to test crossing over along the entire length of the *2L* chromosome arm, as well as across the centromere (see *Materials and Methods* for chromosomal position of markers). We found no reduction in total crossing over in *usp7 RNAi*^{III} females compared to controls (115% of control levels); however, the crossover distribution was shifted toward the centromere (Table 3). Similar *X* chromosome-specific defects on the *X* chromosome with minimal effects on *X* chromosome segregation and shifted crossover distribution on the autosomes have been observed before in hypomorphic mutants of the major SC protein C(3)G(4) (*Discussion*). While these results explain why the rate of *X* chromosome ND is low for *usp7 RNAi*^{III}, they do not explain why *usp7 RNAi*^{II} females have considerably higher missegregation, which suggests that crossovers could be additionally affected on the autosomes in *usp7 RNAi*^{II} (see below).

Table 2. Effect on *X* chromosome recombination frequency and ND in *usp7* RNAi females

	X chromosome interval								
Genotype*	*sc-cv* (% of control)	*cv-f* (% of control)	Total (% of control)	n	% NCO	% SCO	% DCO	Adj N (N)	% *X* ND
+	10.4 (100)	36.3 (100)	46.7 (100)	1,700	55.0	43.3	1.7	3,330 (3,324)	0.4
usp7RNAi^{II}	7.3 (70)	10.7 (29)	18.1† (39)	177	81.9	18.7	0.0	473 (390)	35.1‡
usp7RNAi^{III}	4.8 (46)	15.7 (43)	20.5† (44)	2,096	80.2	19.1	0.7	4,297 (4,202)	4.4‡

*All females were *y w nanos-Gal4::VP16/ y sc cv v f-y+* with either no RNAi construct (+) or the indicated *usp7* RNAi construct. Only the markers *sc*, *cv*, and *f* were scored in female progeny when crossed to *y sc cv v f-car* males. (n) number of females assayed for *X* chromosome recombination from the progeny of 43 (+), 52 (*usp7 RNAi*^{II}), and 58 (*usp7 RNAi*^{III}) females (*SI Appendix*, Table S1). NCO, SCO, and DCO refer to non, single, or double crossovers. Adj N is the adjusted total progeny scored in the ND assay and accounts for the inviable progeny class (*Materials and Methods*). N is the number of progeny before adjusting.

†A chi-square test, analyzing the total number of crossovers verses the total number of non-crossovers, indicates that recombination in both *usp7 RNAi* oocytes is significantly different from control ($P < 0.001$) but not significantly different from each other ($P = 0.5801$). The total number of crossovers:noncrossovers is 765:935 for control, 32:145 for *usp7 RNAi*^{II}, and 415:1681 for *usp7 RNAi*^{III}.

‡Nondisjunction levels are significantly different from control ($P < 0.001$). See Methods for statistical analysis.

Table 3. Effect on *2nd* chromosome recombination frequency in *usp7* RNAi females

Genotype*	*2nd* chromosome interval: *net- dpp^{ho}* (% of control)	*dpp^{ho}-dpy* (% of control)	*dpy-b* (% of control)	*b-pr* (% of control)	*pr-cn* (% of control)	Total (% of control)	N
+	4.97 (100)	7.02 (100)	25.9 (100)	8.55 (100)	3.06 (100)	49.01 (100)	784
usp7RNAi^{III}	4.56 (92)	5.05 (72)	18.2 (70)	24.9 (291)	3.91 (127)	56.29 (115)	614†

*Females were *y w nanos-Gal4::VP16/ naryagfp^{crispr}; net dpp^{ho} dpy b pr cn/+* with either no RNAi construct (+) or the indicated *usp7* RNAi construct. Single female virgins (33 for control and 34 for *usp7RNAi^{III}*) were crossed to *X/Y; net dpp^{ho} dpy b pr cn* males. Only female progeny were scored for the markers *net*, *dpp^{ho}*, *dpy*, *b*, *pr*, and *cn*. (N) is the total number of females scored.
†A chi-square test, analyzing the total number of crossovers verses the total number of noncrossovers, indicates that *usp7 RNAi^{III}* oocytes are not significantly different from control ($P = 0.128$). The total number of crossovers:noncrossovers is 351:433 for control and 300:314 for *usp7 RNAi^{III}*.

Direct Cytogenetic Evaluation of Homolog Co-orientation at Prometaphase I. Unfortunately, the *2nd* chromosome recombination assay yields fewer progeny than the *X* recombination assay, with an average of 40% fewer scorable progeny for the control and *usp7 RNAi^{III}*. Because of this we were unable to test *2nd* chromosome recombination in fertility-compromised *usp7 RNAi^{II}* females by the classical genetic approach (The number of scorable progeny produced by *usp7 RNAi^{II}* for *X* recombination was only ~3/tester female compared to 40 for control and 36 for *usp7 RNAi^{III}* females). To ascertain whether autosomal crossing over was reduced in *usp7 RNAi^{II}* females, we analyzed homolog co-orientation and DNA mass morphologies in prometaphase I oocytes. Females that have reduced crossing over on all chromosomes fail to produce enough chiasmata required to align and hold homologs along the prometaphase I spindle and instead have maloriented homologs that are separated by significant distance (34). We used fluorescence in situ hybridization (FISH) probes that recognized heterochromatic regions of the *X*, *2nd*, *3rd*, and *4th* chromosomes to determine the co-orientation of each chromosome in prometaphase I. Examples of prometaphase I *X* and *4th* chromosome orientation are shown in *SI Appendix*, Fig. S4*A*; examples of *2nd* and *3rd* chromosome orientation are shown in *SI Appendix*, Fig. S4*B*; and DNA mass morphology images are shown in *SI Appendix*, Fig. S4*C* (see *SI Appendix* for details).

Consistent with the low levels of ND and chromosome crossover frequencies on the *X* (Table 2) and *2nd* (Table 3) chromosomes, co-orientation of homologs in *usp7 RNAi^{III}* was only mildly affected (96%, 90%, 90%, and 83% compared to 100%, 100%, 100%, and 89% in controls were properly co-oriented for *X*, *2nd*, *3rd*, and *4th* chromosomes, respectively) (Fig. 2). However, *usp7 RNAi^{II}* prometaphase I oocytes had a much higher percentage of maloriented homologs compared to either control or *usp7 RNAi^{III}* females (only 63%, 57%, 46%, and 76% were properly co-oriented for *X*, *2nd*, *3rd*, and *4th* chromosome, respectively). [Note that the less than complete *4th* chromosome co-orientation in wild-type females is expected due to their dynamic nature on the meiosis I spindle (35).]

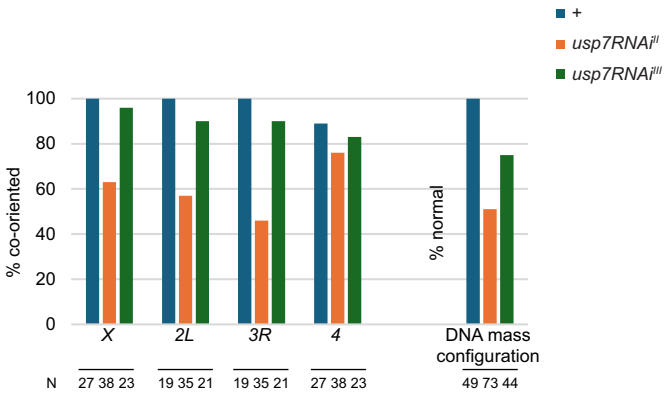

Fig. 2. Homolog orientation by FISH in *usp7 RNAi* prometaphase I oocytes. Quantification of homolog orientation in *y w nanos-Gal4/y sc cv v f-y+* with either no RNAi construct (+, blue) or the indicated *usp7 RNAi* construct (*usp7 RNAi^{II}*, orange or *usp7 RNAi^{III}*, green) using a probe to the *X* (359 repeat), *2L* (AATAG), *3R* (Dodeca), and *4th* chromosome (AATAT). DNA mass configuration was analyzed by DAPI. See *SI Appendix*, Fig. S4 for representative immunofluorescence images. N, number of oocytes analyzed for each probe or prometaphase I DNA mass configuration.

In addition to the inability of *usp7 RNAi^{II}* to co-orient homologs properly, these females also failed to hold homologs at the prometaphase I mid-spindle almost 50% of the time, compared to control and *usp7 RNAi^{III}* which aligned properly 100% and 75% of the time, respectively (Fig. 2). These data indicate that *usp7 RNAi^{II}* females suffer significant reductions in crossing over on both the *X* and autosomes, and it is that failure (and subsequent nonhomologous segregations) that results in the elevated levels of ND observed specifically in this genotype.

Effect of *usp7 RNAi* on Nonexchange Chromosome Segregation. As shown in Table 2, despite similar effects of the two constructs on *X* chromosomal crossing over, *usp7 RNAi^{II}* oocytes exhibit a much higher rate of ND compared to *usp7 RNAi^{III}* oocytes. To further test the idea the effects of *usp7* depletion on segregation are not a reflection of the differences in *X* recombination frequency distribution observed between the two lines, we tested the effects of our two shRNA constructs on *X* chromosome ND in oocytes where the occurrence of crossing over is strongly suppressed by heterozygosity for the *FM7 X* chromosome balancer (36, 37). Despite removal of exchange as a variable between the *usp7 RNAiI^{II}* and *usp7 RNAi^{III}* genotypes, the level of *X* chromosome ND is approximately 15-fold higher in *usp7 RNAiI^{II} X/FM7* females than it is in *usp7 RNAi^{III} X/FM7* females (Table 4). In addition, we observed a significant increase in *4th* chromosome achiasmate ND in *usp7 RNAiI^{II}*, as well as recovered progeny that phenotypically appear to be meiosis II exceptions.

These observations are easily explained by the difference in the effects of the two constructs on autosomal recombination. Oocytes expressing the *usp7 RNAi^{III}* construct show relatively low levels of *X* ND, presumably a consequence of the high levels of autosomal crossing over. The presence of only one pair of nonexchange chromosomes allows the "distributive systems" to segregate nonexchange *X*s in the absence of nonexchange *2nd* and *3rd* chromosomes (33, 36, 38, 39). However, in *usp7 RNAiI^{II}* oocytes there is a global effect on crossing over that created both nonexchange *X* chromosomes and nonexchange autosomes. The presence of multiple nonexchange chromosomes overloads the distributive system, leaving it incapable of properly segregating the nonexchange *X* chromosomes. As a result, nonhomologous segregations (for example both *X* chromosomes segregate from one autosome, *XX<~>A*, with the remaining autosome segregating at random) occur at high frequency. These heterologous segregation events result in the high levels of *X* chromosome ND, in both meiosis I and meiosis II, observed in Tables 2 and 4.

To rule out that any reduction in *usp7* expression beyond the germarium was the cause of the variance in ND, we assayed *X* ND when the shRNA constructs were driven by the *matα-Gal4* driver that drives expression after early meiotic prophase events

Table 4. Effect on *X* and *4th* chromosome ND in *usp7* RNAi females with achiasmate *X* chromosomes

Genotype*	N	Adj N	% *X* ND	% *4th* ND	MII exceptions§
FM7a/+	815	817	0.2	0.0	0
FM7a/+; usp7RNAi^{II}	567	853	29.5†	5.2†	16
FM7w/+;; usp7RNAi^{III}	923	944	2.1‡	0.1¶	0

*The following genotypes were *y w nanos-Gal4::VP16/ FM7a or FM7w* with either no RNAi construct (+) or the indicated *usp7* RNAi construct. Female progeny were crossed to *X^Y, In(1)EN,v f B; C(4)RM,ci ey^{R}* males and females and males were scored for both *X* and *4th* ND. Only *4th* chromosome nullo-exceptions are presented in the table. The total number of progeny scored (N) is adjusted to account for the inviable progeny class (Adj N) (*Materials and Methods*).
†ND levels are significantly different from control ($P < 0.001$).
‡ND levels are significantly different from control ($P < 0.05$).
§Female progeny that resulted from meiosis II (MII) exceptions (phenotypically carried 2 copies of 1 of their female parents *X* chromosomes) were not included when calculating the levels of ND.
¶Not significantly different from control ($P > 0.05$). See *Materials and Methods* for statistical analysis.

(*SI Appendix*, Figs. S2 and S5). We found that reducing *usp7* expression after early/mid-pachytene had no effect on either SC maintenance (*SI Appendix*, Fig. S5*A*) or on the proper segregation of homologs during meiosis I (*SI Appendix*, Fig. S5*B*), indicating that Usp7 expression is specifically required during the early events in the germarium for the disjunction of homologs. These observations allow us to conclude that the effects of these constructs on segregation are best explained by their effects of crossing over.

The Observed Reductions in Crossing Over Are Not a Result of Failed DSB Induction. The recombination phenotype observed when *usp7* expression is reduced, especially in *usp7 RNAi^{II}* females which fail to form enough chiasmata to biorient homologs along the prometaphase I spindle, could be explained by a role of Usp7 in DSB formation and/or repair. To test this, we analyzed DSB formation and repair kinetics is *usp7 RNAi* females from early to mid-pachytene (see *SI Appendix*, Fig. S2 for timing of events). We found, by immunofluorescence analysis, that DSBs are formed and repaired with normal kinetics (Fig. 3 and *SI Appendix*, Fig. S6) indicating that the recombination defects observed in *usp7 RNAi* females are not due to the absence or failure in the timely repair of DSBs. In addition, from the studies shown in Fig. 3, in which we used the cytoplasmic Orb protein to help locate the SC depleted mid-pachytene oocyte, we can determine that there is also no observable defect in cyst development and oocyte specification, as Orb concentrates around a single nucleus in the mid-pachytene cyst.

The SC Maintenance Phenotype Is Not Dependent on DSB Formation. While DSB formation and repair is unaltered when *usp7* expression is decreased, it is possible that a process related to DSBs, for example, meiotic recombination, is directly responsible for the mechanism relating to the failed maintenance of the SC.

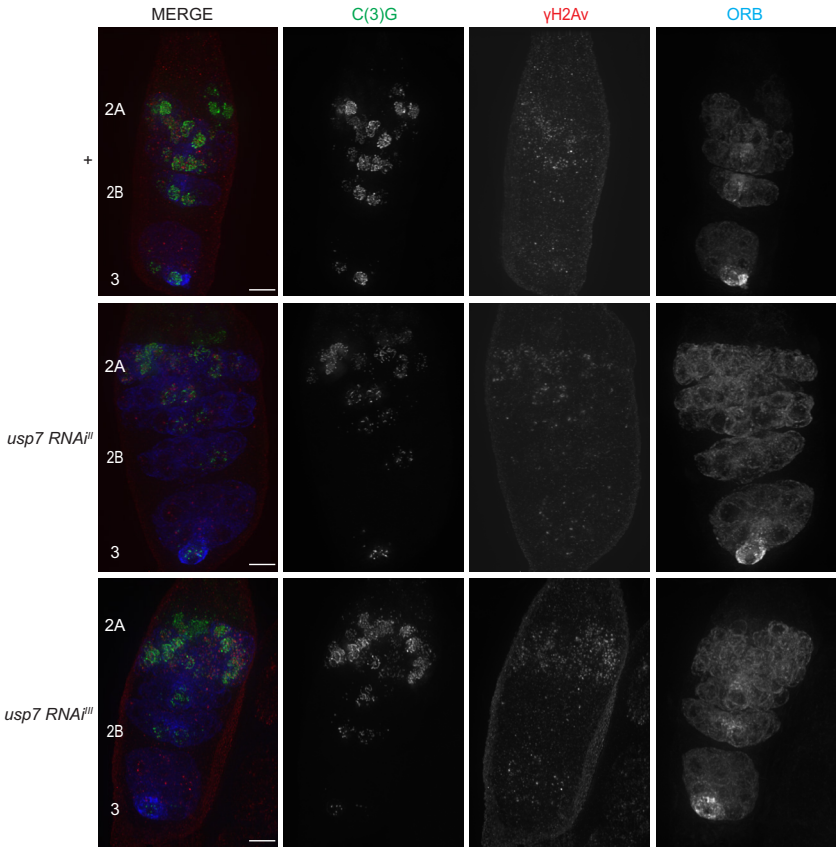

Fig. 3. DSB formation and repair kinetics are globally unaltered in *usp7 RNAi* germaria using a germline driver. Immunofluorescence analysis of whole mount germarium from control (+) and *usp7 RNAi* females (*usp7 RNAi^{II}* or *usp7 RNAi^{III}*) showing DSB formation and repair kinetics are unaltered in *usp7 RNAi* females. Germaria from the three genotypes are all similarly orientated, and early pachytene, early/mid-pachytene, and mid-pachytene cysts are labeled as region 2A, 2B, and 3, respectively. Germarium are stained with antibodies to C(3)G (green) to mark the SC, γH2Av (red) to mark the histone modification of phosphorylation at DSBs, and Orb (blue) to assay developmental defects and to mark the mid-pachytene (region 3) oocyte. (Scale bar, 5 μm.) See *SI Appendix*, Fig. S6 for γH2Av foci quantification throughout the germaria.

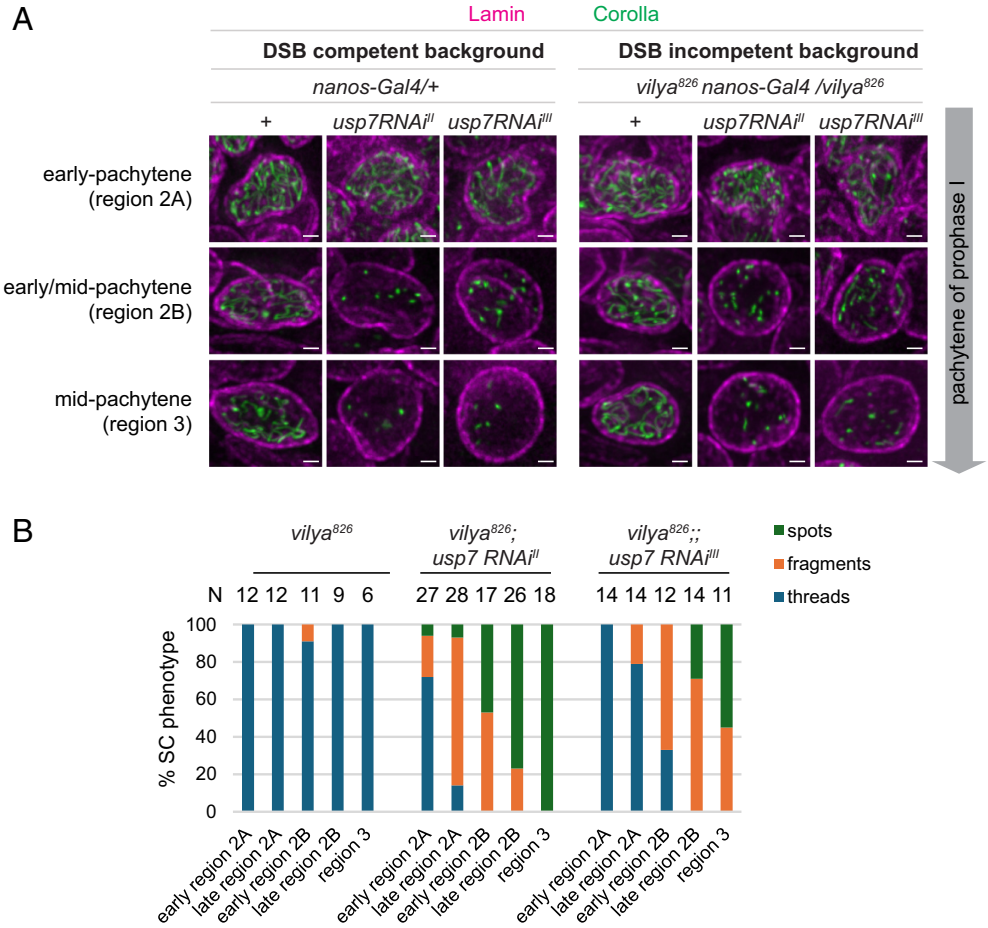

Fig. 4. SC phenotype of *usp7 RNAi* females is independent of the meiotic recombination process. (*A*) Immunofluorescence analysis of nuclei from a DSB competent background (*y w nanos-Gal4/y sc cv v f-y+*) and a DSB incompetent background (*y w vilya^{826} nanos-Gal4/vilya^{826}*) from control (+) and *usp7 RNAi* (*usp7 RNAi^{II}* or *usp7 RNAi^{III}*) females. Ovaries were stained with antibodies to Lamin (magenta) to mark nuclear envelope and Corolla (green) to mark the SC and are shown from meiotic stages of early pachytene (region 2A), early/mid-pachytene (region 2B), and mid-pachytene (region 3). Images are maximum-intensity projections of the deconvolved *z*-series though the selected nuclei. (Scale bar, 1 μm.) (*B*) Quantification of the SC phenotype in *y w vilya^{826} nanos-Gal4/vilya^{826}* with either no RNAi construct (*vilya^{826}*) or the indicated *usp7 RNAi* construct (*vilya^{826}; usp7 RNAi^{II}* or *vilya^{826};; usp7 RNAi^{III}*) throughout early pachytene (early and late region 2A), early/mid-pachytene (early and late region 2B), and mid-pachytene (region 3). N, number of nuclei analyzed for SC phenotype based on C(3)G staining.

Therefore, we combined the knockdown of *usp7* with a mutation in a gene that is required for the formation of DSBs, *vilya* (Fig. 4). We found that the SC maintenance phenotype in *usp7 RNAi* females is independent of the meiotic recombination process, as the SC phenotype is both present and similar in the DSB competent and DSB incompetent backgrounds (Fig. 4*A*). In addition, these results show that the entire SC fails to be maintained, as two components of the SC, C(3)G (Fig. 1*A*) and Corolla (Fig. 4*A*), show similar SC defects throughout pachytene (Fig. 4*B*, compare to Fig. 1*B*).

Taken together, these combined studies suggest that the recombination and ND phenotype observed in *usp7 RNAi* females are a direct consequence of the failure to maintain the SC structure throughout critical stages of pachytene. In the absence of proper SC maintenance, exchange occurs much less frequently which results in increased ND. To further understand the role of Usp7 in SC assembly and maintenance, we chose to study the effects of these shRNA constructs in a context of PC formation, which is independent of homolog–homolog interactions such as pairing and crossing over.

PC Formation Is Affected in *usp7 RNAi^{II}* Oocytes. To determine whether Usp7 may have a direct role in SC structure, we took advantage of loss-of-function mutations in *sina*, an E3 ubiquitin ligase that regulates SC formation and disassembly (11). *sina* mutations result in the formation of large PCs that are heterogenous SC structures that form in early pachytene and persist into late prophase I (11) (*Materials and Methods*). We hypothesized that if we saw changes within the PC structure and/or PC number, this could indicate that Usp7 plays a direct role in the formation of the SC. Specifically, we set out to determine whether *usp7 RNAi^{II}*, the stronger of the two shRNAs, influenced *sina* PC formation. Reduction of Usp7 by *usp7 RNAi^{II}* in the background of *sina* mutations showed PC formation is indeed abnormal (Fig. 5 *A*–*C*). When *usp7* expression is reduced, the *sina* PCs appear thinner throughout the germarium. The large, often tapered, cone-shaped PCs normally found in *sina^{A4}/sina^{Df}* are not present when *usp7* is reduced. A detailed analysis of *sina* PC number, length, and width from early/mid-pachytene to mid/late-pachytene identified that while the number and length of PCs in the germarium are not affected in *usp7 RNAi^{II}* ($P > 0.05$), the width of the PCs formed is significantly affected throughout pachytene when coupled with *usp7 RNAi^{II}* ($P < 0.001$) (Fig. 5 *B* and *E*). These results suggest that Usp7 may be directly acting on an SC component rather than the resulting SC phenotype being due to a downstream effect on chromatin.

Discussion

Regulation of Key Events in Meiosis. The meiotic cell cycle is highly regulated from its entry to its exit through the regulation of cyclin-dependent kinases (40). In addition, specific events throughout meiosis are tightly regulated in both time and space.

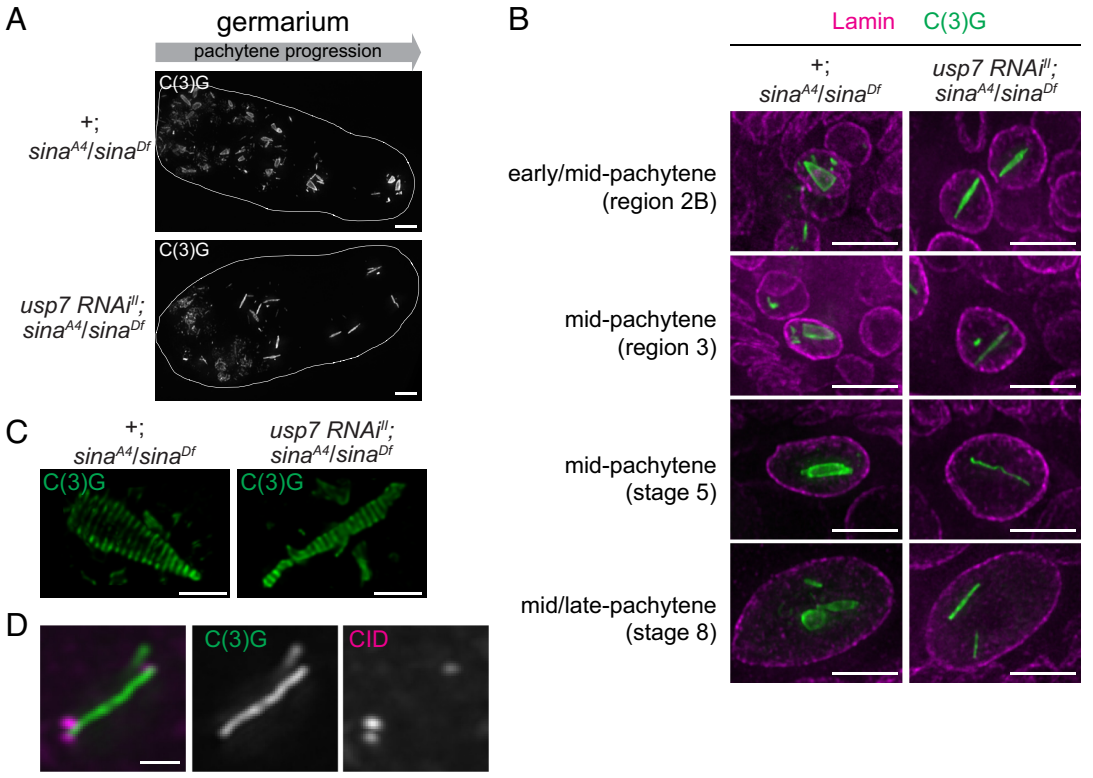

E

Genotype	PC Number				PC size (μm)					
	Region 2B (early/mid-pachytene)		Region 3 (mid-pachytene)		Region 2B (early/mid-pachytene)			Region 3 (mid-pachytene)		
	N	Number	N	Number	N	Length	Width	N	Length	Width
+; *sina*^{A4}/*sina*^{Df}	20	2.35 ± 1.50	10	1.90 ± 1.20	36	2.08 ± 1.00	0.83 ± 0.44	15	1.90 ± 0.81	1.55 ± 0.31
usp7RNAi^{II}; *sina*^{A4}/*sina*^{Df}	15	2.27 ± 1.03	10	1.80 ± 1.14	27	2.24 ± 1.01	0.34 ± 0.13*	16	2.40 ± 1.07	2.40 ± 0.14*

Fig. 5. *sina*-induced PC width is diminished in *usp7 RNAi*^{II} females. (*A*–*E*) Analysis of PC formation from *y w nanos-Gal4/y* or *w* with either no RNAi construct (+) or *usp7 RNAi*^{II} in *sina*^{A4}/*sina*^{Df}. (*A*) Immunofluorescence image of the entire germarium showing PC formation (C(3)G, white) throughout pachytene. (Scale bar, 5 μm.) (*B*) Individual nuclei from early/mid-pachytene (region 2B) through mid/late-pachytene (stage 8 egg chambers) stained with antibodies to Lamin (magenta) to mark nuclear envelope and C(3)G (green) to mark the SC. Images are maximum-intensity projections of the deconvolved *z*-series though the selected nuclei. (Scale bar, 5 μm.) (*C*) Individual nuclei from early/mid-pachytene pro-oocytes stained with C(3)G (green) showing PC structure by high-resolution imaging in the indicated genotypes. (Scale bar, 1 μm.) (*D*) Individual nuclei from early/mid-pachytene pro-oocytes stained with C(3)G (green) and CID (magenta) showing centromere association with *sina* induced PCs in *usp7 RNAi*^{II} oocytes. (Scale bar, 1 μm.) (*E*) Quantification of the number, length, and width of PCs in early/mid-pachytene (region 2B) and mid-pachytene (region 3). N, number of oocytes analyzed for each stage. Number, the average number of PCs per nuclei. SD is in parentheses. * denotes width in *usp7 RNAi*^{II} is significantly different from control ($P < 0.001$) (statistical test, two-tailed Mann–Whitney test).

For example, the SC, a key meiosis-specific structure, which is required for meiotic processes including DSB formation, meiotic recombination, and chromosome segregation [all of which are also regulated posttranslationally (2, 9, 41, 42)], is regulated both in its formation and disassembly (43). In this manuscript, we have uncovered a layer of regulation of the SC in *Drosophila* by the deubiquitinase Usp7. Using RNAi knockdown we showed that *usp7* is required for SC maintenance, a function that is independent of the meiotic recombination process, and likely affecting the SC structure directly. These studies allowed us to study the importance of the SC at specific time points during meiotic prophase and provided strong evidence that maintaining the SC through early/mid-pachytene was essential for the normal level and placement of crossovers.

Deubiquitinase Usp7 and Its Role in Gametogenesis. While small posttranslational protein modifiers like ubiquitination and sumoylation are known to be important for SC formation and meiotic recombination (2, 9, 41, 42), the process of deubiquitination has not been extensively studied as a potential regulator of meiotic prophase. In general, Usp7 is one of the most well-studied deubiquitinases due to its diverse cellular functions and its role in regulating cellular levels of p53, a tumor suppressor protein. As a cysteine peptidase, plays roles in transcriptional regulation, cell cycle progression, DNA damage response, DNA replication, and epigenetic regulation (16, 44). Because of Usp7's p53-dependent role in tumor suppression, as well as its p53-independent role in triple-negative breast cancers, substantial research has focused on finding inhibitors of Usp7 for therapeutic use (45–47).

Several DUBs have been shown to play a role in spermatogenesis, including Usp7 (48). In mice pachytene spermatocytes, Usp7 localizes to the *XY* body in a SCML2 (testes-specific polycomb protein)-specific manner which likely aids in mediating transcriptional silencing. In the absence of SCML2, Usp7 fails to load at the *XY* body, which indirectly leads to an upregulation of histone H2A monoubiquitination and subsequent apoptosis. This action of Usp7 is thought to directly occur through the regulation of RNF2, an E3 ubiquitin ligase (49–51).

Given the diverse roles and overall importance of Usp7, studying its function during specific cellular events can be difficult. Although *usp7* is an essential gene, in *Drosophila*, we circumvented its essential roles in growth and development by specifically downregulating its presence using shRNA constructs driven in a tissue specific manner. Using the *Gal4-UAS* system to knockdown expression in the female and male germlines (*nanos-Gal4*), we were able to show that when there was a greater than 50% reduction in *usp7* germline expression (*usp7 RNAi*^{II}), there was a significant reduction in female fertility. This same construct when assayed for male fertility led to virtual sterility, indicating a role for Usp7 in spermatogenesis. From our data, we conclude that *usp7* likely has a diverse set of functions in both the female and male germlines.

As we will discuss below, the SC maintenance phenotype observed in *usp7 RNAi* oocytes is separable from the effects on fertility in both sexes. *Drosophila* males do not form SC, nor recombine. Thus, the defects observed in males cannot be due to effects on SC assembly or structure. In addition, we showed that in delaying the knockdown of *usp7* from starting in the germarium (where the SC and crossovers are established) to beginning in the vitellarium (*matα-Gal4*), showed that the decrease in fertility is due to a postpachytene role of *usp7* in the vitellarium stages of oogenesis or in early embryos. Further studies will be required to identify whether Usp7 is involved in transcriptional silencing or apoptosis in the *Drosophila* male germline or in the vitellarium in the female germline.

Usp7's Role in Prophase I in *Drosophila* Oocytes. Using immunofluorescence analyses, we showed that Usp7 is required for the maintenance of the SC during prophase I. Although these studies cannot discern the precise knockdown level of *usp7* at each stage of pachytene in the germarium, we hypothesize that the overall differences between the two shRNA constructs correlate with the differences in the timing of the SC defect we observed. Regardless of whether the overall decrease in germline expression was >50% (in *usp7 RNAi*^{II}) or ~10% (in *usp7 RNAi*^{III}), the following observations were the same: 1) tripartite SC structure is able to form; 2) the SC progressively falls apart as the pro-oocytes proceeds though pachytene in the germarium; 3) the resulting SC phenotype in the oocyte by mid-pachytene was indistinguishable; 4) homologous centromeres are paired; and 5) DSB induction was normal. We also showed that the meiotic recombination process was not required to observe the SC phenotype found when *usp7* was reduced. However, knockdown of *usp7* starting in the germarium (*nanos-Gal4*) was required, as there was no SC maintenance phenotype when knockdown began in the vitellarium (*matα-Gal4*) (compare Fig. 1*A* and *SI Appendix*, Fig. S5*A*).

Because the initiation of the meiotic recombination process was not altered nor required for the *usp7 RNAi* phenotype, and centromere pairing remained intact even in the stronger of the two shRNA lines, we concluded that the failure to maintain the SC structure was not a result of gross effects on cohesion. For that reason, we investigated whether Usp7 might directly be affecting an SC component required for the formation and/or maintenance of the SC by analyzing whether reduced *usp7* expression altered the ability to form large SC PCs in a *sina* mutant, which could point to a more direct role in SC formation and/or maintenance. We found that when *usp7* expression is reduced, *sina* induced PC form and appear organized, but they are not able to form the elaborate structures normally found in this genetic background, like cones and complex shapes. While we currently do not know the substate for either the ubiquitin ligase Sina or the deubiquitinase Usp7 regarding their roles in SC formation and maintenance, an intriguing possibility is that they act upon the same substrate(s) to modulate their activity. Future studies will need to be done to address this possibility.

Taken together with the finding that normally structured SC forms prior to it coming apart in most *usp7 RNAi* germaria, we speculate that Usp7 may be required to stabilize, through the action of deubiquitination, a component of the SC or its connection to the lateral element. We cannot exclude the possibility that the effect could be along the lateral elements of the SC, as alterations in *sina* PC structure has also been observed in a *c(2)M* mutant, albeit in length not width (11). The idea the Usp7 is stabilizing a component of the SC is further strengthened by our finding that 83% of the *sina* induced PC in *usp7 RNAi* oocytes were associated with one or more CID foci (39/47 PC analyzed) (Fig. 5*D*), indicating that the SC at the centromeres might be less affected than the SC along the euchromatic arms. Which component is the direct target of Usp7 remains to be determined, as many of the known components of the SC and lateral elements in *Drosophila melanogaster*, C(3)G, Cona, Corolla, and C(2)M, all contain multiple motifs for Usp7 docking based on eukaryotic linear motif (ELM) prediction (*SI Appendix*). Nonetheless, these studies show that when Usp7 is reduced, the SC structure either between homologs or in aberrant PC structures is not able to form and/or maintain long extensions of SC.

SC Function during Critical Time Points in Meiotic Prophase. Although the reduction of *usp7* expression by *usp7 RNAi*^{II} reduced fecundity, fertility was not so affected that it prohibited the analysis of offspring in some genotypes. Through our analysis of the genetic outcomes, we found that *usp7 RNAi*^{II} females show high levels of ND and reduced recombination and altered crossover placement on the *X* chromosome. Our studies analyzing the rates of ND when females have achiasmate *X* chromosomes, in addition to the inability of *usp7 RNAi*^{II} oocytes to biorient their homologs properly at metaphase I, indicate a global reduction in the ability to form crossovers. Supporting this finding is the result that offspring from *usp7 RNAi*^{II} females resulted in meiosis II exceptions, which we speculate are from preceding meiosis I errors. These combined studies suggest that the failure to maintain the SC throughout the time DSBs are initiated (early pachytene) is important for both recombination processes and proper disjunction of homologs. On the other hand, *usp7 RNAi*^{III} females showed only a modest increase in ND, reduced recombination but normal distribution of crossovers on the *X* chromosome, and normal levels of crossovers that are shifted toward the centromeres on one of the autosomes, the *2nd* chromosome. These females were also able to biorient all their homologs, which suggests that recombination rates on the autosomes are likely also not significantly affected. These results show that the ability to maintain the SC throughout early/mid-pachytene is critical for normal levels of crossovers, specifically on the *X* chromosome, and placement of crossovers on the autosomes.

Studies from our lab and many others indicate temporal events that occur between early, early/mid, and mid-pachytene could explain the differences observed in the requirements of the SC at these stages. For instance, DSB induction occurs immediately after SC formation in flies, at early pachytene, and the largest number of DSBs are visualized at this stage when using an antibody to the phosphorylation event that occurs immediately following DSB formation (γH2Av) (8, 52, 53). However, DSB formation and repair is very dynamic, and even in wild-type conditions only a subset of the DSBs that form are ever visualized (8). This indicates that DSB repair is occurring at the same time DSBs are being formed. By the time the pro-oocytes reach early/mid-pachytene, the number of DSBs has been reduced to the number of crossover events, as they colocalize with the recombination nodule components Vilya and Narya (54, 55). We would predict that a failure of the SC to be maintained at

this stage would have significant global effects on crossover and noncrossover formation. Unfortunately, to date, the only proteins in flies that have been physically visualized at sites of recombination are themselves also found at DSB sites in both the future oocyte and pro-oocytes that are disassembling their SC as they back out of meiosis (54). Therefore, we are not confident that we can distinguish sites for recombination from DSBs that have failed to undergo repair when the SC is fragmented, as it is in *usp7 RNAi* females.

A recent study also highlights the importance of maintaining the SC throughout pachytene in *Drosophila* and shows that disruptions of the SC at critical time points affect the *X* chromosome differently than the autosomes (4). Using small deletions in the major transverse filament protein, C(3)G, that differ in when they affect SC structure, it was shown that there are critical times during which you need to maintain the SC. Using these mutants, a timeline was generated for when the SC is necessary to maintain pairing and support the recombination landscape on each of the chromosomes. These mutants suggest that the *X* chromosome requires the SC earlier than the autosome for pairing and crossing over and failure to maintain the SC in early/mid-pachytene alters only the recombination landscape on the autosomes. Our study is consistent with this timeline of full-length SC requirements. However, what has yet to be determined is whether any of these proteins, the C(3)G mutants or Usp7, directly affect the shift in crossovers toward the centromere on the autosomes. We favor the hypothesis that mutations that affect both the level and placement of *X* chromosome crossovers and only alter the distribution of crossovers on the autosomes may reflect an interchromosomal effect, rather than directly altering the position of the crossovers toward the centromere (37, 56, 57).

Materials and Methods

***Drosophila* Genetics.** *Drosophila* strains were maintained on standard food at 24 °C. Descriptions of genetic markers and chromosomes can be found at http://www.flybase.org/. In all figures and tables, (+) denotes the genotype *y w nanos-Gal4/ y sc cv v f ·y+*, *usp7 RNAi^{II}* denotes the genotype *y w nanos-Gal4/ y sc cv v f ·y+; usp7 RNAi^{II}/+*, and *usp7 RNAi^{III}* denotes the genotype *y w nanos-Gal4/ y sc cv v f ·y+; +/+; usp7 RNAi^{III}/+*, unless otherwise indicated. Stocks used in this study can be found in *SI Appendix*.

RNAi Constructs and qPCR. An RNAi hairpin for *usp7* was identified using http://www.flyrnai.org/cgi-bin/RNAi_find_primers.pl. The sequence identified (CACGTGCCCGGATTAAGCATTTGTT) (underlined below) is in the first exon and had no predicted off-targets. The hairpin was cloned using the oligos 5′-ctagcagtCACGTGCCCGGATTAAGCATTTGTTtagttatattcaagcataaACAAATGCTTAATCCGGGCACGTGgcg-3′ and 5′-aattcgcCACGTGCCCGGATTAAGCATTTGTTtatgcttgaatataactaaACAAATGCTTAATCCGGGCACGTGactg-3′ (IDT) into *pValium20* vector (https://fgr.hms.harvard.edu/trip-plasmid-vector-sets) (gift from Jian-Quan Ni and Norbert Perrimon), https://fgr.hms.harvard.edu/trip-plasmid-vector-sets.

qPCR was performed as previously described (54), except that the Tecan Freedom Evo (Tecan Life Sciences) was used to prepare the plates. See *SI Appendix* for detailed methods.

Meiotic ND, Recombination, and Fertility Assays. The frequencies of meiotic ND and meiotic recombination on the *X* chromosome were measured as previously described (54). To assay both *X* and *4th* chromosome ND, tester female virgins were crossed to *X^Y, In(1)EN,v f B; C(4)RM,ci ey^{R}* males. Calculations were performed as previously described (38, 39). Statistical test described in ref. 32. See *SI Appendix* for method details.

To assay for female fertility, single virgin females were crossed to three males (*y sc w+ cv v f · car/B[S]Y*) and allowed to mate for 5 d before parents were removed. Prior to removal of parents, vials were analyzed for death of the female. Only females that survived until day 5 were used to determine the average number of progeny per fly. The number of progeny was recorded for 18 d postmating. To assay for male fertility, single males were mated to single virgin females (*FM7a* for 5 d before parents were removed. Prior to removal of parents, vials were analyzed for death of either parent and noted accordingly. The number of progeny was recorded for 18 d postmating.

Immunostaining and Oocyte Staging. Germaria preparation for whole-mount immunofluorescence was performed as previously described (55). Staging of oocytes was conducted as before (4, 55, 58) using both position and the morphological changes of the cyst. See *SI Appendix* for details of methods and antibodies used.

Imaging and Image Analysis. All images, except Fig. 4*C* and *SI Appendix*, Fig. S3, were acquired using a DeltaVision Elite system (Applied Precision/Leica Microsystems) supplied with a 1 × 70 inverted microscope with a high-resolution CCD camera. Images were deconvolved using SoftWoRx v. 7.2.1 (Applied Precision/GE Healthcare) software. Fig. 4*C* and *SI Appendix*, Fig. S3 images were acquired using Elyra 7 microscope. Image analysis was performed using either SoftWoRx v. 7.2.1 or Imaris software 9.6.1 (Bitplane, Zurich, Switzerland) and cropped in Adobe Photoshop. Brightness and contrast were adjusted minimally to visualize signals during figure preparation.

Interaxis distance was measured using images acquired from the Elyra 7 microscope by similar methods reported in (4, 59, 60). See *SI Appendix* for detailed methods.

For the scoring of PC number in the *sina* mutant, only PCs with clearly defined shapes were scored. No foci/puncta or track-like structures were included in the scoring of PC number. The measurements for length and width of PCs were obtained using SoftWoRx v. 7.2.1 software two-point measurement function in the deconvolved images.

FISH. See *SI Appendix* for detailed methods.

Analysis of Usp7 Docking Site. See *SI Appendix* for detailed methods.

Data, Materials, and Software Availability. All original data have been deposited in Stowers Original Data Repository (https://www.stowers.org/research/publications/libpb-2410). All other data are included in the manuscript and/or *SI Appendix*. Previously published data were used for this work (26).

ACKNOWLEDGMENTS. We would like to thank members of the Hawley lab and Katherine Billmyre for helpful comments and discussion on this project and Angela Miller for illustrations in *SI Appendix*, Fig. S2. We would like to thank the Transgenic RNAi project at Harvard Medical School (NIH/NIGMS R01-GM084947) for providing the transgenic RNAi fly stock used in this study and the Bloomington Stock Center (NIH-P400D018537) for the distribution of stocks. R.S.H is an American Cancer Society Research Professor.

1. S. I. Nagaoka, T. J. Hassold, P. A. Hunt, Human aneuploidy: Mechanisms and new insights into an age-old problem. *Nat. Rev. Genet.* **13**, 493–504 (2012).
2. D. Zickler, N. Kleckner, Recombination, pairing, and synapsis of homologs during meiosis. *Cold Spring Harb. Perspect. Biol.* **7**, a016626 (2015).
3. S. L. Page, R. S. Hawley, The genetics and molecular biology of the synaptonemal complex. *Annu. Rev. Cell Dev. Biol.* **20**, 525–558 (2004).
4. K. K. Billmyre *et al.*, X chromosome and autosomal recombination are differentially sensitive to disruptions in SC maintenance. *Proc. Natl. Acad. Sci. U.S.A.* **116**, 21641–21650 (2019).
5. B. de Massy, Initiation of meiotic recombination: How and where? Conservation and specificities among eukaryotes. *Annu. Rev. Genet.* **47**, 563–599 (2013).
6. F. Baudat, K. Manova, J. P. Yuen, M. Jasin, S. Keeney, Chromosome synapsis defects and sexually dimorphic meiotic progression in mice lacking Spo11. *Mol. Cell* **6**, 989–998 (2000).
7. P. J. Romanienko, R. D. Camerini-Otero, The mouse Spo11 gene is required for meiotic chromosome synapsis. *Mol. Cell* **6**, 975–987 (2000).
8. S. Mehrotra, K. S. McKim, Temporal analysis of meiotic DNA double-strand break formation and repair in *Drosophila* females. *PLoS Genet.* **2**, e200 (2006).
9. S. E. Hughes, D. E. Miller, A. L. Miller, R. S. Hawley, Female meiosis: Synapsis, recombination, and segregation in *Drosophila melanogaster*. *Genetics* **208**, 875–908 (2018).
10. D. E. Miller, Synaptonemal complex-deficient *Drosophila melanogaster* females exhibit rare DSB Repair events, recurrent copy-number variation, and an increased rate of de novo transposable element movement. *G3 (Bethesda)* **10**, 525–537 (2020).
11. S. E. Hughes *et al.*, The E3 ubiquitin ligase Sina regulates the assembly and disassembly of the synaptonemal complex in *Drosophila* females. *PLoS Genet.* **15**, e1008161 (2019).
12. P. Barbosa *et al.*, SCF-Fbxo42 promotes synaptonemal complex assembly by downregulating PP2A-B56. *J. Cell Biol.* **220**, e202009167 (2021).
13. M. K. Jo, K. Rhee, K. P. Kim, S. Hong, Yeast polyubiquitin unit regulates synaptonemal complex formation and recombination during meiosis. *J. Microbiol.* **60**, 705–714 (2022).

14. Y. Wang *et al.*, FBXW24 controls female meiotic prophase progression by regulating SYCP3 ubiquitination. *Clin. Transl. Med.* **12**, e891 (2022).
15. L. Zhou *et al.*, Ubiquitin-specific peptidase 7: A novel deubiquitinase that regulates protein homeostasis and cancers. *Front. Oncol.* **11**, 784672 (2021).
16. A. Pozhidaeva, I. Bezsonova, USP7: Structure, substrate specificity, and inhibition. *DNA Repair (Amst)* **76**, 30–39 (2019).
17. G. J. Valles, I. Bezsonova, R. Woodgate, N. W. Ashton, USP7 is a master regulator of genome stability. *Front. Cell Dev. Biol.* **8**, 717 (2020).
18. T. Zhang, G. Periz, Y. N. Lu, J. Wang, USP7 regulates ALS-associated proteotoxicity and quality control through the NEDD4L-SMAD pathway. *Proc. Natl. Acad. Sci. U.S.A.* **117**, 28114–28125 (2020).
19. J. Q. Ni *et al.*, A genome-scale shRNA resource for transgenic RNAi in *Drosophila*. *Nat. Methods* **8**, 405–407 (2011).
20. L. Cui *et al.*, Deubiquitinase USP7 regulates *Drosophila* aging through ubiquitination and autophagy. *Aging (Albany NY)* **12**, 23082–23095 (2020).
21. M. V. Doren, A. L. Williamson, R. Lehmann, Regulation of zygotic gene expression in *Drosophila* primordial germ cells. *Curr. Biol.* **8**, 243–246 (1998).
22. M. A. Haseeb, A. C. Bernys, E. E. Dickert, S. E. Bickel, An RNAi screen to identify proteins required for cohesion rejuvenation during meiotic prophase in *Drosophila* oocytes. *G3 (Bethesda)* **14**, jkae123 (2024).
23. P. Rørth, Gal4 in the *Drosophila* female germline. *Mech. Dev.* **78**, 113–118 (1998).
24. K. A. Weng, C. A. Jeffreys, S. E. Bickel, Rejuvenation of meiotic cohesion in oocytes during prophase I is required for chiasma maintenance and accurate chromosome segregation. *PLoS Genet.* **10**, e1004607 (2014).
25. A. M. Hudson, L. Cooley, Methods for studying oogenesis. *Methods* **68**, 207–217 (2014).
26. S. Takeo, C. M. Lake, E. Morais-de-Sá, C. E. Sunkel, R. S. Hawley, Synaptonemal complex-dependent centromeric clustering and the initiation of synapsis in *Drosophila* oocytes. *Curr. Biol.* **21**, 1845–1851 (2011).
27. N. Christophorou, T. Rubin, J. R. Huynh, Synaptonemal complex components promote centromere pairing in pre-meiotic germ cells. *PLoS Genet.* **9**, e1004012 (2013).
28. N. S. Tanneti, K. Landy, E. F. Joyce, K. S. McKim, A pathway for synapsis initiation during zygotene in *Drosophila* oocytes. *Curr. Biol.* **21**, 1852–1857 (2011).
29. R. Yan, B. D. McKee, The cohesion protein SOLO associates with SMC1 and is required for synapsis, recombination, homolog bias and cohesion and pairing of centromeres in *Drosophila* meiosis. *PLoS Genet.* **9**, e1003637 (2013).
30. M. R. Gyuricza *et al.*, Dynamic and stable cohesins regulate synaptonemal complex assembly and chromosome segregation. *Curr. Biol.* **26**, 1688–1698 (2016).
31. B. Krishnan *et al.*, Sisters unbound is required for meiotic centromeric cohesion in *Drosophila melanogaster*. *Genetics* **198**, 947–965 (2014).
32. Y. Zeng, H. Li, N. M. Schweppe, R. S. Hawley, W. D. Gilliland, Statistical analysis of nondisjunction assays in *Drosophila*. *Genetics* **186**, 505–513 (2010).
33. B. S. Baker, J. C. Hall, "Meiotic mutants: Genetic control of meiotic recombination and chromosome segregation" in *The Genetics of Biology of Drosophila*, M. Ashburner, E. Novitski, Eds. (Academic Press, New York, NY, 1976), vol. 1a, pp. 351–434.
34. K. S. McKim, J. Ko Jang, W. E. Theurkauf, R. Scott Hawley, Mechanical basis of meiotic metaphase arrest. *Nature* **362**, 364–366 (1993).
35. S. E. Hughes *et al.*, Heterochromatic threads connect oscillating chromosomes during prometaphase I in *Drosophila* oocytes. *PLoS Genet.* **5**, e1000348 (2009).
36. D. E. Miller, K. R. Cook, R. S. Hawley, The joy of balancers. *PLoS Genet.* **15**, e1008421 (2019).
37. H. Li *et al.*, Heterozygous inversion breakpoints suppress meiotic crossovers by altering recombination repair outcomes. *PLoS Genet.* **19**, e1010702 (2023).
38. R. S. Hawley *et al.*, There are two mechanisms of achiasmate segregation in *Drosophila* females, one of which requires heterochromatic homology. *Dev. Genet.* **13**, 440–467 (1992).
39. A. E. Zitron, R. S. Hawley, The genetic analysis of distributive segregation in *Drosophila melanogaster*. I. Isolation and characterization of Aberrant X segregation (Axs), a mutation defective in chromosome partner choice. *Genetics* **122**, 801–821 (1989).
40. I. Palacios-Blanco, C. Martín-Castellanos, Cyclins and CDKs in the regulation of meiosis-specific events. *Front. Cell Dev. Biol.* **10**, 1069064 (2022).
41. M. Ito, A. Shinohara, Chromosome architecture and homologous recombination in meiosis. *Front. Cell Dev. Biol.* **10**, 1097446 (2022).
42. G. V. Börner, A. Hochwagen, A. J. MacQueen, Meiosis in budding yeast. *Genetics* **225**, iyad125 (2023).
43. C. K. Cahoon, R. S. Hawley, Regulating the construction and demolition of the synaptonemal complex. *Nat. Struct. Mol. Biol.* **23**, 369–377 (2016).
44. R. Rawat, D. T. Starczynowski, P. Ntziachristos, Nuclear deubiquitination in the spotlight: The multifaceted nature of USP7 biology in disease. *Curr. Opin. Cell Biol* **58**, 85–94 (2019).
45. J. Yi *et al.*, Inhibition of USP7 induces p53-independent tumor growth suppression in triple-negative breast cancers by destabilizing FOXM1. *Cell Death Differ.* **30**, 1799–1810 (2023).
46. Y. T. Lin *et al.*, USP7 induces chemoresistance in triple-negative breast cancer via deubiquitination and stabilization of ABCB1. *Cells* **11**, 3294 (2022).
47. R. I. Oliveira, R. A. Guedes, J. A. R. Salvador, Highlights in USP7 inhibitors for cancer treatment. *Front. Chem.* **10**, 1005727 (2022).
48. Y. Xiong, C. Yu, Q. Zhang, Ubiquitin-proteasome system-regulated protein degradation in spermatogenesis. *Cells* **11**, 1058 (2022).
49. M. Luo *et al.*, Polycomb protein SCML2 associates with USP7 and counteracts histone H2A ubiquitination in the XY chromatin during male meiosis. *PLoS Genet.* **11**, e1004954 (2015).
50. P. de Bie, D. Zaaroor-Regev, A. Ciechanover, Regulation of the Polycomb protein RING1B ubiquitination by USP7. *Biochem. Biophys. Res. Commun.* **400**, 389–395 (2010).
51. D. U. Menon, Y. Shibata, W. Mu, T. Magnuson, Mammalian SWI/SNF collaborates with a polycomb-associated protein to regulate male germline transcription in the mouse. *Development* **146**, dev174094 (2019).
52. J. K. Jang, D. E. Sherizen, R. Bhagat, E. A. Manheim, K. S. McKim, Relationship of DNA double-strand breaks to synapsis in *Drosophila*. *J. Cell Sci.* **116**, 3069 (2003).
53. H. Liu, J. K. Jang, N. Kato, K. S. McKim, mei-P22 encodes a chromosome-associated protein required for the initiation of meiotic recombination in *Drosophila melanogaster*. *Genetics* **162**, 245–258 (2002).
54. C. M. Lake *et al.*, Narya, a RING finger domain-containing protein, is required for meiotic DNA double-strand break formation and crossover maturation in *Drosophila melanogaster*. *PLoS Genet.* **15**, e1007886 (2019).
55. C. M. Lake *et al.*, Vilya, a component of the recombination nodule, is required for meiotic double-strand break formation in *Drosophila*. *eLife* **4**, e08287 (2015).
56. K. N. Crown, D. E. Miller, J. Sekelsky, R. S. Hawley, Local inversion heterozygosity alters recombination throughout the genome. *Curr. Biol.* **28**, 2984–2990.e3 (2018).
57. A. H. Sturtevant, A case of rearrangement of genes in *Drosophila*. *Proc. Natl. Acad. Sci. U.S.A.* **7**, 235–237 (1921).
58. E. R. Wesley, R. S. Hawley, K. K. Billmyre, Genetic background impacts the timing of synaptonemal complex breakdown in *Drosophila melanogaster*. *Chromosoma* **129**, 243–254 (2020).
59. Y. Xiang *et al.*, Multiple reorganizations of the lateral elements of the synaptonemal complex facilitate homolog segregation in *Bombyx mori* oocytes. *Curr. Biol.* **34**, 352–360.e4 (2024).
60. C. K. Cahoon *et al.*, Superresolution expansion microscopy reveals the three-dimensional organization of the *Drosophila* synaptonemal complex. *Proc. Natl. Acad. Sci. U.S.A.* **114**, E6857–E6866 (2017).